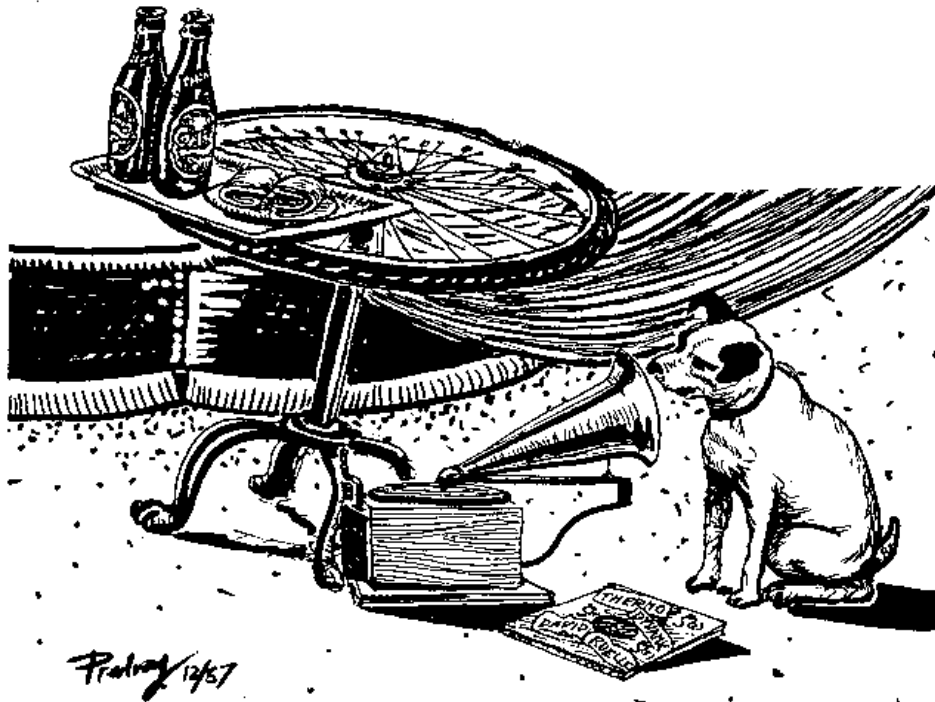# Chaos: Classical and Quantum
Part I: Deterministic Chaos

Predrag Cvitanović – Roberto Artuso – Ronnie Mainieri – Gregor Tanner – Gábor Vattay – Niall Whelan – Andreas Wirzba
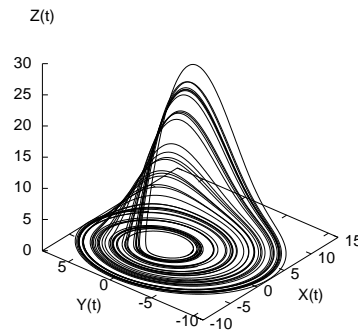
Figure 2.3: A trajectory of the Rössler flow at time $t = 250$. (G. Simon)

x_q is an *equilibrium point* (often referred to as a *stationary, fixed,* or *stagnation* point), and the trajectory remains forever stuck at x_q. Otherwise the trajectory passing through x_0 at time $t = 0$ can be obtained by integrating the equations (2.5):

$$x(t) = f^t(x_0) = x_0 + \int_0^t d\tau \, v(x(\tau)), \qquad x(0) = x_0. \qquad (2.8)$$

We shall consider here only *autonomous* flows, that is, flows for which the velocity field v_i is *stationary*, not explicitly dependent on time. A non-autonomous system

$$\frac{dy}{d\tau} = w(y, \tau), \qquad (2.9)$$

can always be converted into a system where time does not appear explicitly. To do so, extend ("suspend") phase space to be $(d + 1)$-dimensional by defining $x = \{y, \tau\}$, with a stationary vector field

$$v(x) = \begin{bmatrix} w(y, \tau) \\ 1 \end{bmatrix}. \qquad (2.10)$$

The new flow $\dot{x} = v(x)$ is autonomous, and the trajectory $y(\tau)$ can be read off $x(t)$ by ignoring the last component of x.

Example 2.2 A flow with a strange attractor: *The Duffing flow of figure 2.2 is bit of a bore - every trajectory ends up in one of the two attractive equilibrium points. Let's construct a flow that does not die out, but exhibits a recurrent dynamics. Start with a harmonic oscillator*

$$\dot{x} = -y, \qquad \dot{y} = x. \qquad (2.11)$$

The solutions are Ae^{it}, Ae^{-it}, and the whole x-y plane rotates with constant angular velocity $\theta = 1$, period $T = 2\pi$. Now make the system unstable by adding

$$\dot{x} = -y, \qquad \dot{y} = x + ay, \qquad a > 0. \qquad (2.12)$$

The plane is still rotating with constant angular velocity, but trajectories are now spiraling out. In general, any flow in the plane either escapes, falls into an attracting equilibrium point, or converges to a limit cycle - richer dynamics requires at least one more dimension. In order to prevent the trajectory from escaping to ∞, kick it into 3rd dimension when x reaches some value c by adding

$$\dot{z} = b + z(x - c)\,, \qquad c > 0\,. \tag{2.13}$$

Now z shoots upwards exponentially, $z \simeq e^{(x-c)t}$. In order to bring it back, start decreasing x by modifing its evolution equation to

$$\dot{x} = -y - z\,.$$

Large z drives the trajectory toward $x = 0$; there the exponential contraction by e^{-ct} kicks in, and the trajectory drops back toward the x-y plane. This frequently studied example of an autonomous flow is called the Rössler *system (for definitiveness we fix the parameters a, b, c in what follows):*

$$
\begin{aligned}
\dot{x} &= -y - z \\
\dot{y} &= x + ay \\
\dot{z} &= b + z(x - c)\,, \qquad a = b = 0.2\,, \quad c = 5.7\,.
\end{aligned}
\tag{2.14}
$$

The system is as simple as they get - it would be linear, were it not for the sole bilinear term zx. Even for so "simple" a system the nature of long-time solutions is far from obvious.

There are two repelling equilibrium points:

$$
\begin{aligned}
(x^-, y^-, z^-) &= (\,0.0070,\, -0.0351,\, 0.0351\,) \\
(x^+, y^+, z^+) &= (\,5.6929,\, -28.464,\, 28.464\,)
\end{aligned}
\tag{2.15}
$$

One is close to the origin by construction - the other, some distance away, must exist because the equilibrium has a 2nd-order nonlinearity.

To see what other solutions look like we need to resort to numerical integration. A typical numerically integrated long-time trajectory is sketched in figure 2.3. As we shall show in sect. 4.1, for this flow any finite volume of initial conditions shrinks with time, so the flow is contracting. Trajectories that start out sufficiently close to the origin seem to converge to a strange attractor. We say "seem", as there exists no proof that such an attractor is asymptotically aperiodic - it might well be that what we see is but a long transient on a way to an attractive periodic orbit. For now, accept that figure 2.3 and similar figures in what follows are examples of "strange attractors". (continued in exercise 2.8)   *(Rytis Paškauskas)*

2.3   Computing trajectories

> On two occasions I have been asked [by members of Parliament], 'Pray, Mr. Babbage, if you put into the machine wrong figures, will the right answers come out?' I am not able rightly to apprehend the kind of confusion of ideas that could provoke such a question.
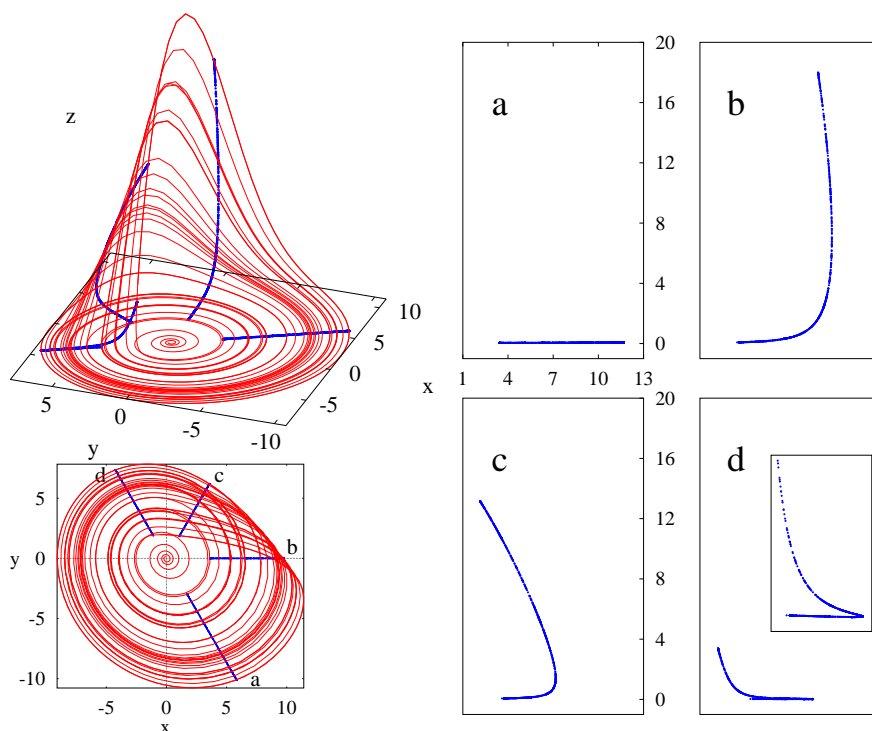> Charles Babbage

Figure 3.1: (Right:) a sequence of Poincaré sections of the Rössler strange attractor, defined by planes through the z axis, oriented at angles (a) -60° (b) 0°, (c) 60°, (d) 120°, in the x-y plane. (Left:) side and x-y plane view of trajectory with Poincaré sections superimposed. (Rytis Paškauskas)

point traces a trajectory through this phase space. As long as the motion is oscillatory, in the pendulum all orbits are loops, so any trajectory will periodically intersect the line, that is the Poincaré section, at one point.

Consider next a pendulum with friction, such as the unforced Duffing system plotted in figure 2.2. Now every trajectory is an inward spiral, and the trajectory will intersect the Poincaré section $y = 0$ at a series of points that get closer and closer to either of the equilibrium points; the Duffing oscillator at rest.

Motion of a pendulum is so simple that you can sketch it yourself on a piece of paper. The next example (as well as example **??**) offers a better illustration of the utility of visualization of dynamics by means of Poincaré sections.

Example 3.3 Rössler attractor: *Consider figure 2.3, a typical trajectory of the 3-dimensional Rössler flow (2.14). It wraps around the z axis, so a good choice for a Poincaré section is a plane passing through the z axis. A sequence of such Poincaré sections placed radially at increasing angles with respect to the x axis, figure 3.1, illustrates the "stretch & fold" action of the Rössler flow. To orient yourself, compare this with figure 2.3, and note the different z-axis scales. Figure 3.1 assembles these sections into a series of snapshots of the flow. A line segment $[A, B]$, traversing the width of the attractor, starts out close to the x-y plane, and after the stretching (a) $\rightarrow$ (b) followed by the folding (c) $\rightarrow$ (d), the folded segment returns close to the x-y plane strongly compressed. In one Poincaré return the $[A, B]$ interval is stretched, folded and mapped onto itself, so the flow is* expanding. *It is also* mixing, *as in one Poincaré return the point C from the interior of the attractor is mapped into the outer edge, while the edge point B lands in the interior.*
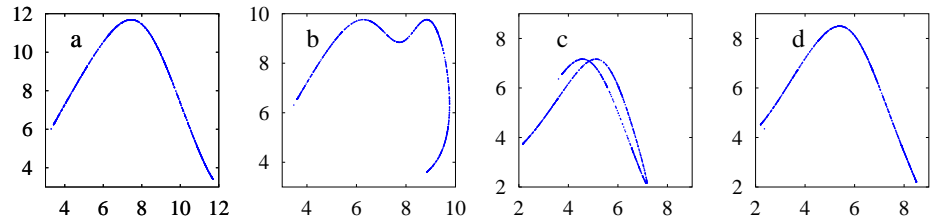
Figure 3.2: Return maps for the $R_n \rightarrow R_{n+1}$ radial distance Poincaré sections of figure 3.1. (Rytis Paškauskas)

Once a particular Poincaré section is picked, we can also exhibit the return map (3.1), as in figure 3.2. Cases (a) and (d) are examples of nice 1-to-1 return maps. However, (b) and (c) appear multimodal and non-invertible, artifacts of projections of a 2-dimensional return map $(R_n, z_n) \rightarrow (R_{n+1}, z_{n+1})$ onto a 1-dimensional subspace $R_n \rightarrow R_{n+1}$. (continued in exercise 3.1)

fast track:

sect. 3.3, p. 49

The above examples illustrate why a Poincaré section gives a more informative snapshot of the flow than the full flow portrait. For example, while the full flow portrait of the Rössler flow figure 2.3 gives us no sense of the thickness of the attractor, we see clearly in the Rössler Poincaré sections figure 3.1 that even though the return map is 2-d → 2-d, the flow contraction is so strong that for all practical purposes it renders the return map 1-dimensional.

3.2 Constructing a Poincaré section

☞ remark 3.1

For almost any flow of physical interest a Poincaré section is not available in analytic form. We describe here a numerical method for determining a Poincaré section.

Consider the system (2.5) of ordinary differential equations in the vector variable $x = (x_1, x_2, \ldots, x_d)$

$$\frac{dx_i}{dt} = v_i(x, t), \tag{3.6}$$

where the flow velocity v is a vector function of the position in phase space x and the time t. In general v cannot be integrated analytically and we will have to resort to numerical integration to determine the trajectories of the system. Our task is to determine the points at which the numerically integrated trajectory traverses a given hypersurface. The hypersurface will

Example 4.4 **Complex stability eigenvalues, diagonal:** *If* **A** *can be brought to the diagonal form, the solution (4.13) to the differential equation (4.8) can be written either as*

$$\begin{pmatrix} x_1(t) \\ x_2(t) \end{pmatrix} = \begin{pmatrix} e^{t\lambda_1} & 0 \\ 0 & e^{t\lambda_2} \end{pmatrix} \begin{pmatrix} x_1(0) \\ x_2(0) \end{pmatrix}, \tag{4.20}$$

or

$$\begin{pmatrix} x_1(t) \\ x_2(t) \end{pmatrix} = e^{t\lambda} \begin{pmatrix} e^{it\theta} & 0 \\ 0 & e^{-it\theta} \end{pmatrix} \begin{pmatrix} x_1(0) \\ x_2(0) \end{pmatrix}. \tag{4.21}$$

In the case $\lambda_1 > 0$, $\lambda_2 < 0$, x_1 grows exponentially with time, and x_2 contracts exponentially. This behavior, called a saddle, *is sketched in figure 4.2(b), as are the remaining possibilities: in/out nodes, inward/outward spirals, and the center. Spirals arise from taking a real part of the action of* $\mathbf{J}^t$ *on a complex eigenvector. The magnitude of $|x(t)|$ diverges exponentially when $\lambda > 0$, and contracts toward 0 when the $\lambda < 0$, whereas the imaginary phase θ controls its oscillations.*

In general $\mathbf{J}^t$ is neither diagonal, nor diagonalizable, nor constant along the trajectory. Still, any matrix, including $\mathbf{J}^t$, can be expressed in the singular value decomposition form

$$\mathbf{J} = \mathbf{UDV}^T$$

where $\mathbf{D}$ is diagonal, and $\mathbf{U}$, $\mathbf{V}$ are orthogonal matrices. The diagonal elements Λ_1, Λ_2, ..., Λ_d of $\mathbf{D}$ are called the *stability eigenvalues*.

Under the action of the flow an infinitesimally small ball of initial points is deformed into an ellipsoid: Λ_i is the relative stretching of the ith principal axis of the ellipsoid, the columns of the matrix $\mathbf{V}$ are the principal axes $\mathbf{e}_i$ of stretching in the Lagrangian coordinate frame, and the orthogonal matrix $\mathbf{U}$ gives the orientation of the ellipse in the Eulerian coordinates.

Now that we have some feeling for the qualitative behavior of eigenvectors and eigenvalues, we are ready to return to the general case: nonlinear flows.

4.3 Stability of flows

How do you determine the eigenvalues of the finite time local deformation $\mathbf{J}^t$ for a general nonlinear smooth flow? The Jacobian matrix is computed by integrating the equations of variations (4.2)

$$x(t) = f^t(x_0), \quad \delta x(x_0, t) = A^t(x_0)\delta x(x_0, 0). \tag{4.22}$$

The equations of variations are linear, so we should be able to integrate them - but in order to make sense of the answer, we derive it step by step.
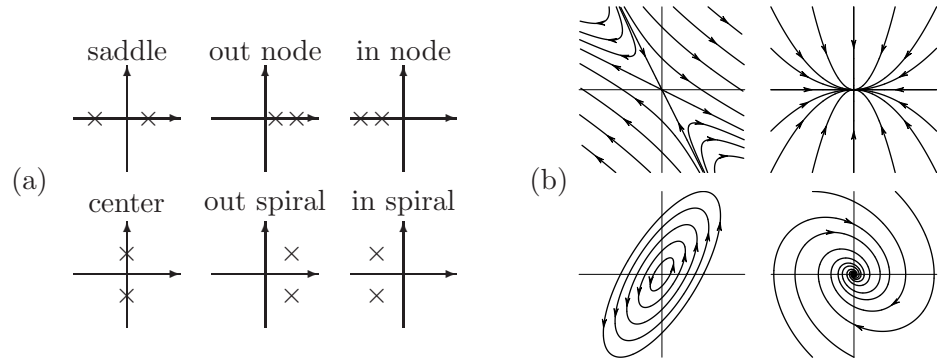
Figure 4.2: (a) Qualitatively distinct types of stability exponents of a $[2\times2]$ stability matrix. (b) Streamlines for several typical 2-dimensional flows: saddle (hyperbolic), in node (attracting), center (elliptic), in spiral.

4.3.1   Stability of equilibria

For a start, consider the case where x_q is an equilibrium point (2.7). Expanding around the equilibrium point x_q, using the fact that the matrix $\mathbf{A} = \mathbf{A}(x_q)$ in (4.2) is constant, and integrating,

$$f^t(x) = x_q + e^{\mathbf{A}t}(x - x_q) + \cdots, \tag{4.23}$$

we verify that the simple formula (4.13) applies also to the Jacobian matrix of an equilibrium point,

$$\mathbf{J}^t(x_q) = e^{\mathbf{A}t} \qquad \mathbf{A} = \mathbf{A}(x_q). \tag{4.24}$$

Example 4.5 Equilibria of the Rössler flow.   *The Rösler system (2.14) has two equilibrium points*

$$(x^-, y^-, z^-) = (\, 0.0070, \, -0.0351, \, 0.0351 \,)$$
$$(x^+, y^+, z^+) = (\, 5.6929, \, -28.4648, \, 28.4648 \,)$$

The two equilibria together their stability exponents now yield quite detailed information about the flow. Figure 4.3 shows two trajectories which start in the neighborhood of the "+" equilibrium point. Trajectories to the right of the "+" equilibrium point escape, and those to the left spiral toward the "−" equilibrium point, where they seem to wander chaoticaly for all times. The stable manifold of "+" equilibrium point thus serves as a attraction basin boundary. Consider now the linearized stability exponents of the two equilibria

$$(\lambda_1^-, \lambda_2^- \pm i\,\theta_2^-) = \quad (-5.686, \qquad\quad 0.0970 \pm i\,0.9951\,)$$
$$(\lambda_1^+, \lambda_2^+ \pm i\,\theta_2^+) = \quad (\,0.1929, \quad -4.596 \times 10^{-6} \pm i\,5.428\,) \tag{4.25}$$

The $\lambda_2^+ \pm i\,\theta_2^+$ complex eigenvalue pair implies that that neighborhood of the outer equilibrium point rotates with angular period $T_+ \approx \left|2\pi/\theta_2^+\right| = 1.1575$. The stability multiplier by which a trajectory that starts near the "+" equilibrium point contracts in the stable manifold plane is the excrutiatingly slow $\Lambda_2^+ \approx \exp(\lambda_2^+ T_+) = 0.9999947$ per rotation. For each period the point of the stable manifold moves away along the unstable